HHS Public Access

Author manuscript

J Magn Reson Imaging. Author manuscript; available in PMC 2020 November 01.

Published in final edited form as:

J Magn Reson Imaging. 2019 November ; 50(5): 1424–1432. doi:10.1002/jmri.26718.

Quantitative multi-voxel proton MR spectroscopy for the identification of white matter abnormalities in mild traumatic brain injury: comparison between regional and global analysis

Matthew S. Davitz, BS[1], **Oded Gonen, PhD**[1], **Assaf Tal, PhD**[2], **James S. Babb, PhD**[1], **Yvonne W. Lui, MD**[1], **Ivan I. Kirov, PhD**[1]

[1]Center for Advanced Imaging Innovation and Research (CAI[2]R), Bernard and Irene Schwartz Center for Biomedical Imaging, New York University School of Medicine, Department of Radiology, 660 1st Avenue, New York, NY 10016, USA

[2]Department of Chemical Physics, Weizmann Institute of Science, Rehovot 7610001, Israel

Abstract

Background: Three-dimensional (3D) brain proton MR spectroscopic imaging (^{1}H MRSI) facilitates simultaneous metabolic profiling of multiple loci, at higher, sub 1 cm^3, spatial resolution than single-voxel ^{1}H MRS with ability to separate tissue-type partial volume contribution(s).

Purpose: To determine if: *(a)* white matter (WM) damage in mild traumatic brain injury (mTBI) is homogeneously-diffuse, or if specific regions are more affected; *(b)* partial-volume corrected, structure-specific ^{1}H MRSI voxel averaging is sensitive to regional WM metabolic abnormalities.

Study type: Retrospective cross-sectional cohort study.

Population: 27 subjects: 15 symptomatic mTBI patients, 12 matched controls.

Field strength/sequence: 3 T using 3D ^{1}H MRSI over a 360 cm^3 volume-of-interest (VOI) centered over the corpus callosum, partitioned into 480 voxels, each 0.75 cm^3.

Assessment: *N*-acetyl-aspartate (NAA), creatine, choline and *myo*-inositol concentrations estimated in predominantly WM regions: body, genu and splenium of the corpus callosum, corona radiata, frontal and occipital WM.

Statistical tests: ANCOVA to compare patients with controls in terms of regional concentrations. The effect sizes (Cohen's *d*) of the mean differences were compared across regions and with previously published global data obtained with linear regression of the WM over the entire VOI in the same dataset.

Results: Despite patients' *global* VOI WM NAA being significantly lower than the controls', no *regional* differences were observed for any metabolite. Regional NAA comparisons, however, were *all* unidirectional (patients' NAA concentration ‹ controls') within a narrow range: 0.3≤ Cohen's *d* ≤0.6.

Corresponding author: Ivan I. Kirov, PhD., Tel.: 212-263-3337, FAX: 212-263-7541, ivan.kirov@nyulangone.org.

Data conclusion: Since the patient group was symptomatic and exhibiting global WM NAA deficits, these findings suggest: *(a)* diffuse axonal mTBI damage; that is *(b)* below the ^{1}H MRSI detection threshold in small regions. Therefore, larger, *i.e.,* more sensitive single-voxel ^{1}H MRS, placed anywhere in WM regions may be well suited for mTBI ^{1}H MRS studies, given that these results are confirmed in other cohorts.

Keywords

MR spectroscopy; multivoxel MRS; traumatic brain injury; white matter; human studies

INTRODUCTION

Mild traumatic brain injury (mTBI), the most common type of head trauma, is a leading public health problem (1). While most victims make full recovery, a subset report persisting post-concussive symptoms (PCS), which result in personal suffering and an estimated $17 billion annual loss for the US economy (2). Currently, there are two main clinical measures of mTBI sequelae: the Glasgow Coma Scale (GCS) score and head CT (3). Both are critical for acute triage, but have no utility thereafter for the typical mTBI patient who reports PCS despite normal neurological (GCS score of 15) and radiological exams. Consequently, a major research focus in mTBI imaging is on approaches that are sensitive to the microscopic damage known to exist in normal-appearing (on CT and clinical (T_1/T_2-weighted) MRI) brain tissue.

Basic science studies have unequivocally established that the most common injury site in TBI of all severities, is the brain's white matter (WM) (4). The sudden change in acceleration associated with a TBI results in mechanical strain which starts a pathological cascade of microstructural, as well as metabolic changes (5). Diffusion tensor imaging (DTI) is well-suited to investigate the former, while proton MR spectroscopy (^{1}H MRS) can potentially detect the latter. Consequently, both techniques have been extensively used in TBI (3, 6).

Transitioning these modalities to the clinic, however, has been stymied by uncertainty as to which of several available regional or global approaches provides the best classification of normal *versus* injured tissue. TBI has been studied with single-voxel (7, 8) ^{1}H MRS (typical size 3.5–8 cm^{3}), and multi-voxel ^{1}H MRSI (9–11) with its typical volumes-of-interest (VOI) ›100 cm^{3}. The latter also facilitates higher spatial resolution, ‹1 cm^{3}, simultaneous acquisition of all loci, and the separation of the white and gray matter (WM, GM) contribution in the entire VOI in post-processing using linear regression (12, 13). The main difficulty with single-voxel methods is inefficiency, examining only one or *sequentially* few loci; and since a single spectrum is obtained from a (relatively) large voxel, discerning its WM from the GM contribution is impossible. The main issue with ^{1}H MRSI is that its smaller voxels' signal-to-noise-ratio (SNR) is often insufficient to detect mTBI changes. Consequently, neither method can easily answer whether mTBI WM pathology is homogeneously-diffuse or multi-focal and if the latter, how many and where those foci might be.

To address this, two ^{1}H MRSI approaches for assessing WM injury are compared in terms of statistical significance and effect size: regional voxel averaging and global linear regression. Previously, with the latter approach we found lower WM *n*-acetyl-aspartate (NAA) in a cohort of symptomatic mTBI patients (14). In the current study we use voxel averaging in the same dataset to study regional WM metabolism. By comparing the results and effect sizes across the different WM regions and to those obtained with global linear regression we aimed to determine if: *(a)* WM damage is homogeneously-diffuse, or if specific regions are more affected; *(b)* partial-volume corrected, structure-specific ^{1}H MRSI voxel averaging is sensitive to regional WM metabolic abnormalities. Answering the questions above would allow us to provide empirical motivation for selecting a particular WM region or post-processing strategy in future studies aiming for maximum sensitivity to WM injury in mTBI.

MATERIALS AND METHODS

Human Subjects

This is a retrospective analysis of data from 15 PCS-positive mTBI patients (mean age 36, range 18–51, four females) and 12 age- and gender-matched controls (mean age 34, range 19–52, four females) for whom global linear regression analysis has been reported (14). Originally these subjects were part of a larger cohort (13), but subsequent dichotomization into PCS-negative and PCS-positive patient groups revealed metabolic differences compared to controls only in the latter (14). Because a cohort with known global injury was needed to test our hypotheses, the current study examined only the PCS-positive patient group. The inclusion criteria were GCS score 15–13, less than 30 minutes loss of consciousness (LOC) and post-traumatic amnesia (PTA) of less than 24 hours. Controls were entered into the study after providing negative answers to a list of disqualifying neurological conditions and reporting no MRI contraindications. The T1- and T2-weighted imaging of all subjects was independently reviewed by a board certified neuroradiologist with certificate of added qualification with 15 years of experience (Y.W.L.), and a neuroimaging researcher with 10 years of experience (I.I.K.). The MRI criteria for including controls into the study were lack of pathologic findings, including stroke, hemorrhage, mass, or other imaging evidence of neurological disease. The study was approved by the Institutional Review Board, and signed informed consent was obtained from all participants.

Data Acquisition

The study was done at 3 T with a transmit-receive head-coil, as described previously (13). Briefly, FLAIR and MPRAGE MRI were used to image-guide the ^{1}H MRSI VOI over the corpus callosum (CC), as shown in Figure 1A-C. Custom auto-shim software then adjusted the scanner's first and second order currents (15). A 10 cm anterior-posterior (AP)×8 cm left-right (LR)×4.5 cm inferior-superior (IS)=360 cm^3 VOI was excited with TE/TR=35/1800 ms PRESS in three second-order Hadamard encoded slabs (6 0.75 cm thick slices,) interleaved every TR along the IS direction, as shown in Figure 1B,C for optimal SNR and spatial coverage (16). The slabs were partitioned with 16×16 (AP×LR) chemical shift imaging, as shown in Figure 1A, yielding 80 voxels, 1.0×1.0×0.75 cm^3 each. At two averages, the ^{1}H MRSI took 34 minutes and the entire protocol just under an hour.

Segmentation

A medical student (M.S.D.) with 2 years of experience in neuroimaging research used freely- available software ("FireVoxel" (17)) to manually outline the corona radiata, CC body, genu and splenium, frontal and occipital WM ROIs on each subject's axial MPRAGE MRI, using DTI atlas parcellations guidance (18), as shown in Figures 1, 2. These six regions have been reported as most commonly injured in TBI, based on previous ^{1}H MRS (6, 19), DTI (20), and histopathology (21–23). Brain GM and CSF masks were segmented with SPM2 (24).

Metabolic quantification

The ^{1}H MRSI data were processed as described previously (13). Phantom replacement was used to convert spectral-fitted line area estimates, using Soher *et al.*'s SIFiTTools (25), into absolute millimolar concentrations. Relaxation times differences between each metabolite *in vivo* (T_1^{vivo}, T_2^{vivo}) and phantom (T_1^{vitro}, T_2^{vitro}), were accounted for by a factor, Λ_i:

$$\Lambda_i = \frac{e^{-TE/T_2^{vitro}}}{e^{-TE/T_2^{vivo}}} \cdot \frac{1-e^{TR/T_1^{vitro}}}{1-e^{-TR/T_1^{vivo}}} \quad (1)$$

The following T_1^{vivo} values reported at 3 T were used for NAA, Cr, Cho and mI: 1360, 1300, 1145, 1170 ms (26). Region-specific T_2^{vivo} values at 3 T were available for NAA, Cr and Cho (average T_2^{vivo} = 374, 185, 238) (27), while for mI, T_2^{vivo} = 200 ms (28) was used for all ROIs. The NAA, Cr, Cho and mI relaxation values in the phantom were T_1^{vitro} = 605, 336, 235, 319 ms and T_2^{vitro} = 483, 288, 200, 233 ms (29).

Spectral quality control comprised excluding the metabolites whose Cramer-Rao lower bounds (CRLB) were ›20% (30); and rejecting "outliers," *i.e.,* exceeding ×3 standard deviations (SD) from the mean of all voxels (31). The global WM metabolic concentrations were obtained with linear regression over all the VOI voxels (12, 13).

Partial volume considerations

Due to the relatively coarse ^{1}H MRSI spatial resolution relative to the sizes and shapes of the investigated regions (See Figures 1, 2), GM and cerebrospinal fluid (CSF) partial volume need to be accounted for. This was achieved in the following manner. All voxels with CSF fraction (f_{CSF}) ›0.3, (causing lower SNR, hence, higher CRLB), were excluded. Metabolic concentrations in the remaining voxels were normalized by dividing by (1-f_{CSF}). To reduce GM signal contributions from adjacent basal ganglia and cortex, all voxels with f_{GM} ›0.3 were also excluded. To ensure sampling of voxels with a predominant WM ROI content, an

acceptance threshold of f_{WM}≥0.5 was applied for the CC structures (higher f_{WM} excluded ›50% of subject data). However, for the larger WM regions, namely the corona radiata, occipital and frontal WM, using f_{WM}≥0.5 included a number of voxels with partial volume of adjacent WM, as well as some GM-containing voxels (0.3› f_{WM} ›0). To counteract this effect, higher thresholds were used for the frontal and occipital WM (f_{WM}›0.7), and for the corona radiata (f_{WM}›0.8). These thresholds were found to best: (*i*) prevent data loss, which would have affected the comparisons with the published global data from these cohorts, while (*ii*) keeping the voxel number as similar as possible across all ROIs, in order to exclude very different measurement precision amongst the regions. Finally, we averaged the metabolites' data from all voxels that survived these criteria *and* fell within the structure mask (see Figure 2A-E).

Statistical analysis

ANCOVA was used to compare patients with controls' metabolite concentrations within each region while adjusting for potential confounding effects of age and gender. For each ROI, the number of voxels in each subject was included in the analysis as a weighting factor in order to adjust for inter-subject variation in the precision with which each metabolite was measured. The error variance was allowed to differ across comparison groups to avoid the assumption of variance homogeneity. The normality assumption underlying each analysis was assessed with a Shapiro-Wilk test to the residuals from each ANCOVA model. Rejection of the assumption of normality for any combination of metabolite and region led to the analysis being repeated with the vector of ranks of metabolite levels in that region being used instead, as dependent variable. There was no one instance where the distribution of the residuals from an analysis based on ranks was found to be significantly different from normal. Cohen's *d*, providing a measure of effect size, was defined as the difference between the concentration means divided by the pooled SD:

$$d = \frac{\bar{X}_p - \bar{X}_c}{\sqrt{\left[\left(n_p - 1\right)S_p^2 + \left(n_c - 1\right)S_c^2\right]} / \left(n_p + n_c - 2\right)} \quad (2)$$

where n_p, n_c, $\bar{X}_p$, $\bar{X}_c$ and S_p, S_c denote the patients' and controls sample size, mean and SD.

Coefficients of variation (CVs = SD/mean ×100%) were calculated. All tests were conducted at the two-sided 5% significance level using SAS 9.3 (SAS Institute, Cary, NC).

RESULTS

Patient demographics, symptoms, MRI findings and duration of LOC and PTA are compiled in Table 1. Sample spectra from one of the six ^{1}H MRSI slices from a patient is shown in Figure 1D. The partial volume and spectra quality control thresholds resulted in voxels for the body of the CC only in 2 controls and 5 patients and therefore this region was excluded

from further analysis. All patients and controls contributed data for each of the other structures, except patient #6 in Table 1, who did not contribute to the genu of the CC, and one control (30 year old male) who did not contribute to frontal WM. Examples of voxel selection based on the outlined ROIs and spectra passing the selection criteria, are shown in Figure 1 for the body of the corpus callosum and corona radiata, and in Figure 2 for the genu, splenium, occipital and frontal WM

The distribution of model residuals was found to be significantly different from the normal distribution for mI in the frontal (p=0.006) and occipital (p=0.006) WM, and for Cho and NAA in the corona radiata (p = 0.011 and 0.026). Therefore, the comparison of patients to controls in terms of these metabolite levels in these WM ROIs was based on ranks.

Controls' and patients' average±SD metabolite concentrations in each ROI, are compiled in Table 2. There were no significant differences between the cohorts in any metabolite in any ROI (all $p \geq 0.2$), even *before* multiple comparisons correction. However, the patients' mean and median NAA concentrations were lower than controls' in all ROIs (Table2 and Figure 3). Cohen's d for these comparisons ranged from 0.3 – 0.6, much smaller than the 1.7 found for statistically significant result of the comparison of these patients' and controls' *global* WM NAA (14).

DISCUSSION

Our focus on WM stems from the knowledge that torsional axonal injury is the most common sequela in TBI of all severities, as shown by *in vitro* and *in vivo* histopathological studies (4, 5). Fortunately, sampling predominantly WM VOIs that are large enough to yield both SNR and reproducibility to detect mTBI metabolic variations, is not technically difficult with the standard, single-voxel ^{1}H MRS sequences which have been available on all major manufacturers' scanners for over two decades. Indeed, a substantial body of the ^{1}H MRS TBI literature has, consequently, focused on WM injury using this technique. Unfortunately, since *(i)* only a single 3–8 cm^{3} VOI is almost always acquired; and *ii)* mTBI rarely, ‹20% of cases, results in MRI-visible pathology to guide that VOI, investigators are forced to make an *ad hoc* assumption where that pathology might be.

This practice led to several confounding obstacles. First, if a pathology is detected, it is impossible to ascertain if the outcome was just incidental or the result of carefully planned placement. This is especially true considering the heterogeneity of the injury location, type and extent. Second, it is impossible to conclude whether other location(s) are also affected and to what extent. Third, due to the low spatial resolution, it is not even possible to ascertain whether *all* the WM in the single-voxel is affected, since if not, the "healthy" WM partial volume will reduce the sensitivity to the fractional pathology. Finally, fourth, it is not possible to ascertain, with single-voxel ^{1}H MRS, whether mTBI damage is homogeneously-diffuse, inhomogeneously-diffuse or discrete multi focal.

^{1}H MRSI, also available for a long time as product sequences on commercial scanners, with its hundreds, even thousands of voxels, over most (even all) the brain, at an order of magnitude better spatial resolution, has, at least theoretically, a potential to address all these

obstacles (32, 33). Unfortunately, this advantage, especially (much) smaller voxels, come at the cost of lower voxel SNR, *i.e.,* sensitivity to changes, perhaps leading to frequent negative or variable findings. This motivated us to restrict our study cohort to mTBI patients with *known* metabolic deficits in a large VOI containing ~40% of their WM (14). The ^{1}H MRSI localization grid in these VOIs, then, allowed us to resample the *same* data and leverage its finer localization, to test whether regional, structure-specific regions, also exhibit detectable differences. This choice narrowed the questions to only that of sufficient sensitivity, not whether or not there is a difference in the first place.

Using linear regression on this dataset, lower global WM NAA was previously found in patients compared to controls (14). Since that approach was by design sensitive to widespread abnormalities (12, 13), it was expected for the current study that most regions would show the same result. Surprisingly, there were no statistically significant differences within *any* WM ROI, but in line with the notion of widespread injury, we observed lower patients' mean and median NAA concentrations in *every* region. This, along with the finding of similar effect sizes across all regions, is consistent with the interpretation that injury was truly homogeneously-diffuse, *i.e.* no region was spared, but also that no region had sufficiently high injury magnitude to yield a statistically significant finding when examined with regional voxel averaging.

The similarity in the Cohen's *d* values was due to the narrow ranges of the numerator and denominator of Eq. [2]: 6%–8% for the difference in average NAA concentrations in patients and controls and 15%–21% for the average CVs of the regional analysis. The implications of these findings are discussed below.

The previous *global* analyses revealed no Cr, Cho or mI abnormalities (14). This could be the outcome of three possible scenarios in a regional analysis: (*i*) no patients - controls differences in *any* region; (*ii*) differences in only few foci, since a global approach is insensitive to changes in a few voxels; (*iii*) multifocal, but variable differences, *e.g.* higher levels in some regions, offset by lower in others, *e.g.,* Cr, reported elevated in the CC (9), but decreased in frontal WM (34). Our results reveal no significant Cr, Cho or mI findings in any region, *i.e.,* scenario *(i)* pertains. In contrast with the NAA, there was no consistent behavior of their concentrations in patients *versus* controls. One possible reason for the lack of Cho findings may be our cohort's "milder" TBI (lower GCS range of 13), compared to the type studied in the ^{1}H MRSI studies reporting increased Cho (lower GCS range of 10 (33) and 6 (35)). It is therefore possible that elevations of Cho indicate a higher level of injury, or are confined to focal GM regions. While it is not clear if Cr changes are to be expected in TBI, the reports of altered levels (9, 10, 33, 35) indicate that both higher and lower concentrations may result, underscoring the caution needed when metabolic ratios with Cr as the denominator are used for quantification.

Studies that examined multiple WM regions support the assertion that, when present, metabolic changes in mTBI patients are widespread and not confined to single regions. Evidence of this was provided as early as the first multivoxel ^{1}H MRSI application in mTBI, which found lower NAA/Cr and higher Cho/Cr in almost all ROIs, but only in a minority of cases were these differences statistically significant (32). These findings were replicated in

two subsequent ^{1}H MRSI publications. In the first one, all eight WM ROIs showed the same trends for these ratios, as well as individually for lower NAA and higher Cho (33). Similarly, only some were significant. Of note, more severe TBI showed the same metabolic pattern, but the differences were of higher magnitude and hence were more often statistically significant (33). While the second study performed a voxel-based, rather than an ROI analysis, the results were again similar: multiple brain regions showed metabolic abnormalities, which were most pronounced in the more disabled patients (35). It is therefore possible that in light of this study, negative findings in regional WM represent lack of statistical power (sensitivity) rather than absent injury.

A major finding of this study was that, compared to regional voxel averaging, global linear regression had better sensitivity to discriminate patients from controls. Together with the finding of similar, small effect sizes in the regional NAA analysis, this suggests that to detect axonal injury, *sensitivity* may be more important than the choice of WM region, *i.e.,* localization. Specifically, the difference in patients' NAA concentration and the controls' in any WM ROI, would have been detected with an approach yielding CVs of 6–8%. This would be achievable with single-voxel ^{1}H MRS (36, 37), which can be used without concern for WM partial volume: if indeed WM injury is relatively homogeneous, small inter-scan differences in voxel placement within pure WM could be inconsequential. Since reproducibility (sensitivity) depends on a number of experimental factors such as single-voxel sequence, scanner magnetic field and fitting software, we cannot recommend a particular voxel size or placement until the results are validated with single-voxel ^{1}H MRS in an independent cohort. However, given these provisos, it may be hypothesized that ~$(6\ \mathrm{cm})^3$ voxel placed carefully (with images on all 3 planes) in the centrum semiovale could be a reasonable choice for studying WM injury in mTBI.

As shown in the current study, *global* approaches may also have a role, since they yield comparable CVs ‹8% (12, 38, 39), due to combining many voxels' data. Given the ^{1}H MRS evidence of diffuse injury in other cohorts (32, 33, 40), global ^{1}H MRSI approaches in TBI are warranted and indeed used (9–11).

We note the following limitations. First, since all mTBI patients were PCS-positive, it is unknown if the results reported herein are also pertinent to cohorts with different clinical presentation, in particular given that metabolic abnormalities may resolve after the resolution of PCS (7). Second, the cohort is composed of patients scanned within a range of 3 to 55 days post-injury, which may reduce the sensitivity of the ^{1}H MRS measurement, since findings are likely to be different as metabolic recovery, or lack thereof, occurs. This heterogeneity may also explain the lack of findings in Cho and mI, metabolites shown to change in other cohorts (6). The above limitations can be addressed in a more complicated longitudinal study with narrower injury ranges and separating the patients in groups of resolved and unresolved PCS. Third, since each structure comprised only few voxels, it was not practical to differentiate GM from WM contribution beyond the f_{WM} criterion. Possible GM fractional-volume may decrease the sensitivity to WM injury. Fourth, although care was taken to prevent head motion during the scan, localization errors due to subtle patient movement are possible given the small volumes of the examined ROIs. In addition, while a 15 patient cohort may seem modest, the finding of lower, albeit not statistically significant

NAA concentrations in all structures will not likely benefit from an increased *N* since: *(i)* the lack of significance may reflect the heterogeneity of the mTBI insult; and *(ii)* group averages while instructive as a characterization, may not be particularly meaningful for individual patients undergoing diagnosis or treatment response monitoring.

In conclusion, regional WM analysis of ^{1}H MRSI data revealed consistent lower NAA concentrations in patients versus controls, with comparable effect sizes across all ROIs, but no statistical significance. Since these cohorts were also (previously) studied with a *global* WM measures, benefiting from much increased sensitivity, the present findings suggest that axonal injury is truly homogeneously-diffuse *not* multi-focal, and that the sensitivity of ^{1}H MRSI at clinical (3 T) field, ‹1 cm^3 voxels and ~half an hour acquisition may be insufficient to detect regional differences in few cm^3 volume typical of WM brain structures. Since single-voxel ^{1}H MRS yielding reproducibility CVs of under 8% would have detected a difference in NAA between patients and controls in any WM ROI, a single voxel ^{1}H MRS VOI, placed anywhere in WM may be the simplest approach for this modality in mTBI. This conjecture has important implications for clinical ^{1}H MRS and therefore should be tested in a new dataset.

Acknowledgments

Grant support: National Institutes of Health (NIH) award numbers NS097494, NS39135, NS090417, MH110418, MH108962 and P41EB017183. The content is solely the responsibility of the authors and does not necessarily represent the official views of the NIH, which had no role in study design; in the collection, analysis and interpretation; the writing of the report; and decision to submit the article for publication.

REFERENCES:

1. National Center for Injury Prevention and Control CfDCaP. Report to Congress on mild traumatic brain injury in the United States: steps to prevent a serious public health problem. Atlanta: Centers for Disease Control and Prevention; 2003.
2. Thurman DJ. The epidemiology and economics of head trauma. New York: John Wiley and Sons; 2001.
3. Shenton ME, Hamoda HM, Schneiderman JS, et al. A review of magnetic resonance imaging and diffusion tensor imaging findings in mild traumatic brain injury. Brain Imaging Behav. 2012;6:137–92. [PubMed: 22438191]
4. Bigler ED. Neuroimaging biomarkers in mild traumatic brain injury (mTBI). Neuropsychol Rev. 2013;23:169–209. [PubMed: 23974873]
5. Johnson VE, Stewart W, Smith DH. Axonal pathology in traumatic brain injury. Exp Neurol. 2013.
6. Lin AP, Liao HJ, Merugumala SK, Prabhu SP, Meehan WP 3rd, Ross BD. Metabolic imaging of mild traumatic brain injury. Brain Imaging Behav. 2012;6:208–23. [PubMed: 22684770]
7. Vagnozzi R, Signoretti S, Cristofori L, et al. Assessment of metabolic brain damage and recovery following mild traumatic brain injury: a multicentre, proton magnetic resonance spectroscopic study in concussed patients. Brain. 2010;133:3232–42. [PubMed: 20736189]
8. Dhandapani S, Sharma A, Sharma K, Das L. Comparative evaluation of MRS and SPECT in prognostication of patients with mild to moderate head injury. J Clin Neurosci. 2014;21:745–50. [PubMed: 24417798]
9. Gasparovic C, Yeo R, Mannell M, et al. Neurometabolite Concentrations in Gray and White Matter in Mild Traumatic Brain Injury: A 1HMagnetic Resonance Spectroscopy Study. J Neurotrauma. 2009.

10. Yeo RA, Gasparovic C, Merideth F, Ruhl D, Doezema D, Mayer AR. A longitudinal proton magnetic resonance spectroscopy study of mild traumatic brain injury. J Neurotrauma. 2011;28:1–11. [PubMed: 21054143]
11. Mayer AR, Ling JM, Dodd AB, Gasparovic C, Klimaj SD, Meier TB. A Longitudinal Assessment of Structural and Chemical Alterations in Mixed Martial Arts Fighters. J Neurotrauma. 2015;32:1759–67. [PubMed: 26096140]
12. Tal A, Kirov II, Grossman RI, Gonen O. The role of gray and white matter segmentation in quantitative proton MR spectroscopic imaging. NMR Biomed. 2012;25:1392–400. [PubMed: 22714729]
13. Kirov II, Tal A, Babb JS, Lui YW, Grossman RI, Gonen O. Diffuse axonal injury in mild traumatic brain injury: a 3D multivoxel proton MR spectroscopy study. J Neurol. 2013;260:242–52. [PubMed: 22886061]
14. Kirov II, Tal A, Babb JS, et al. Proton MR spectroscopy correlates diffuse axonal abnormalities with post-concussive symptoms in mild traumatic brain injury. J Neurotrauma. 2013;30:1200–4. [PubMed: 23339670]
15. Hu J, Javaid T, Arias-Mendoza F, Liu Z, McNamara R, Brown TR. A fast, reliable, automatic shimming procedure using 1H chemical-shift-imaging spectroscopy. J Magn Reson B. 1995;108:213–9. [PubMed: 7670755]
16. Goelman G, Liu S, Hess D, Gonen O. Optimizing the efficiency of high-field multivoxel spectroscopic imaging by multiplexing in space and time. Magn Reson Med. 2006;56:34–40. [PubMed: 16767711]
17. Rusinek H, Glodzik L, Mikheev A, Zanotti A, Li Y, De Leon M. Fully automatic segmentation of white matter lesions: error analysis and validation of a new tool. Intern J Computer Assisted Radiology & Surgery. 2013;8:289–91.
18. Mori S, van Zijl PCM, Oishi K, Faria AV. MRI Atlas of Human White Matter: Elsevier; 2011.
19. Gardner A, Iverson GL, Stanwell P. A systematic review of proton magnetic resonance spectroscopy findings in sport-related concussion. J Neurotrauma. 2014;31:1–18. [PubMed: 24047225]
20. Hulkower MB, Poliak DB, Rosenbaum SB, Zimmerman ME, Lipton ML. A decade of DTI in traumatic brain injury: 10 years and 100 articles later. AJNR Am J Neuroradiol. 2013;34:2064–74. [PubMed: 23306011]
21. Browne KD, Chen XH, Meaney DF, Smith DH. Mild traumatic brain injury and diffuse axonal injury in swine. J Neurotrauma. 2011;28:1747–55. [PubMed: 21740133]
22. Cecil KM, Lenkinski RE, Meaney DF, McIntosh TK, Smith DH. High-field proton magnetic resonance spectroscopy of a swine model for axonal injury. J Neurochem. 1998;70:2038–44. [PubMed: 9572290]
23. Mouzon B, Chaytow H, Crynen G, et al. Repetitive mild traumatic brain injury in a mouse model produces learning and memory deficits accompanied by histological changes. J Neurotrauma. 2012;29:2761–73. [PubMed: 22900595]
24. Ashburner J, Friston K. Multimodal image coregistration and partitioning--a unified framework. Neuroimage. 1997;6:209–17. [PubMed: 9344825]
25. Soher BJ, Young K, Govindaraju V, Maudsley AA. Automated spectral analysis III: application to in vivo proton MR spectroscopy and spectroscopic imaging. Magn Reson Med. 1998;40:822–31. [PubMed: 9840826]
26. Traber F, Block W, Lamerichs R, Gieseke J, Schild HH. 1H metabolite relaxation times at 3.0 tesla: Measurements of T1 and T2 values in normal brain and determination of regional differences in transverse relaxation. J Magn Reson Imaging. 2004;19:537–45. [PubMed: 15112302]
27. Kirov II, Fleysher L, Fleysher R, Patil V, Liu S, Gonen O. Age dependence of regional proton metabolites T2 relaxation times in the human brain at 3 T. Magn Reson Med. 2008;60:790–5. [PubMed: 18816831]
28. Posse S, Otazo R, Caprihan A, et al. Proton echo-planar spectroscopic imaging of J-coupled resonances in human brain at 3 and 4 Tesla. Magn Reson Med. 2007;58:236–44. [PubMed: 17610279]

29. Kirov II, Liu S, Tal A, et al. Proton MR spectroscopy of lesion evolution in multiple sclerosis: Steady-state metabolism and its relationship to conventional imaging. Hum Brain Mapp. 2017;38:4047–63. [PubMed: 28523763]
30. Oz G, Alger JR, Barker PB, et al. Clinical proton MR spectroscopy in central nervous system disorders. Radiology. 2014;270:Appendix E1.
31. Maudsley AA, Domenig C, Govind V, et al. Mapping of brain metabolite distributions by volumetric proton MR spectroscopic imaging (MRSI). Magn Reson Med. 2009;61:548–59. [PubMed: 19111009]
32. Govindaraju V, Gauger GE, Manley GT, Ebel A, Meeker M, Maudsley AA. Volumetric proton spectroscopic imaging of mild traumatic brain injury. AJNR Am J Neuroradiol. 2004;25:730–7. [PubMed: 15140711]
33. Govind V, Gold S, Kaliannan K, et al. Whole-brain proton MR spectroscopic imaging of mild-to-moderate traumatic brain injury and correlation with neuropsychological deficits. J Neurotrauma. 2010;27:483–96. [PubMed: 20201668]
34. Vagnozzi R, Signoretti S, Floris R, et al. Decrease in N-acetylaspartate following concussion may be coupled to decrease in creatine. J Head Trauma Rehabil. 2013;28:284–92. [PubMed: 23249772]
35. Maudsley AA, Govind V, Levin B, Saigal G, Harris L, Sheriff S. Distributions of Magnetic Resonance Diffusion and Spectroscopy Measures with Traumatic Brain Injury. J Neurotrauma. 2015;32:1056–63. [PubMed: 25333480]
36. Terpstra M, Cheong I, Lyu T, et al. Test-retest reproducibility of neurochemical profiles with short-echo, single-voxel MR spectroscopy at 3T and 7T. Magn Reson Med. 2016;76:1083–91. [PubMed: 26502373]
37. Wijtenburg SA, Gaston FE, Spieker EA, et al. Reproducibility of phase rotation STEAM at 3T: focus on glutathione. Magn Reson Med. 2014;72:603–9. [PubMed: 24151202]
38. Gasparovic C, Bedrick EJ, Mayer AR, et al. Test-retest reliability and reproducibility of short-echo-time spectroscopic imaging of human brain at 3T. Magn Reson Med. 2011.
39. McLean MA, Woermann FG, Barker GJ, Duncan JS. Quantitative analysis of short echo time (1)H-MRSI of cerebral gray and white matter. Magn Reson Med. 2000;44:401–11. [PubMed: 10975892]
40. Signoretti S, Marmarou A, Aygok GA, Fatouros PP, Portella G, Bullock RM. Assessment of mitochondrial impairment in traumatic brain injury using high-resolution proton magnetic resonance spectroscopy. J Neurosurg. 2008;108:42–52. [PubMed: 18173309]

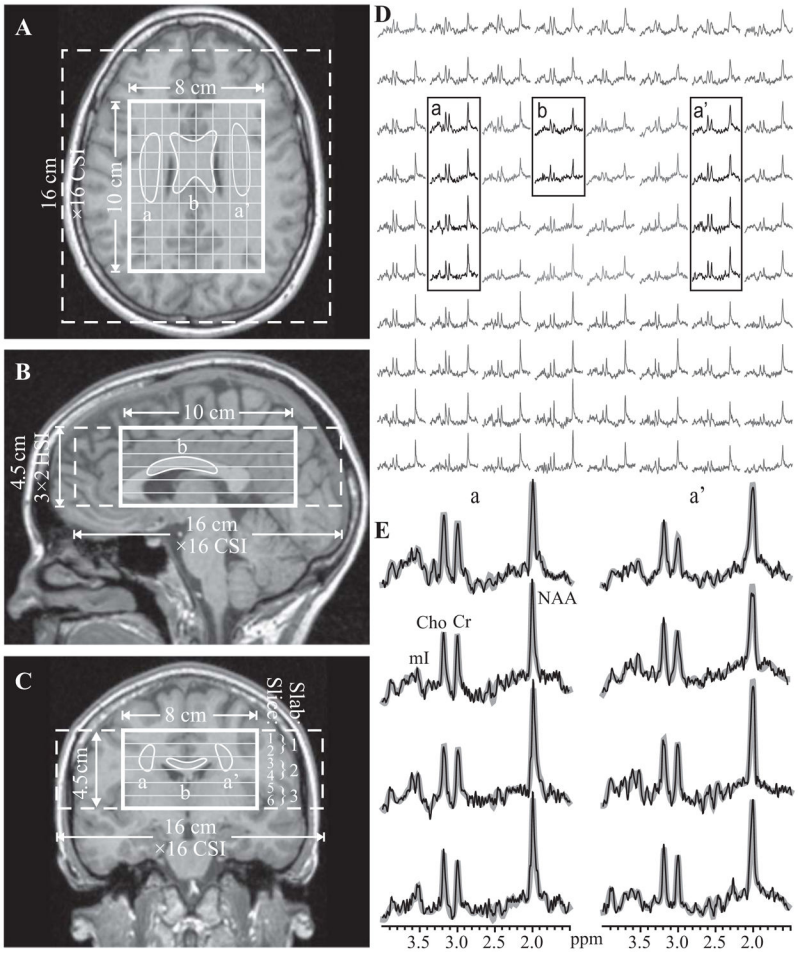

Fig. 1.

Left (**A**-**C**): Patient #12's axial, sagittal and coronal T1-weighted MPRAGE MRI superimposed with the ^{1}H MRSI's FOV, VOI and localization grid (dashed, solid thick and thin white frames) and the outlines of the bilateral corona radiata (**a**, **a'**) and body of the CC (**b**). Right, top (**D**): Real part of the 8×10 (LR×AP) ^{1}H spectra matrix from the spectroscopic slice on **A** (grayed lines). Spectra from the corresponding WM ROIs are in black traces. Right, bottom (**E**): Magnified spectra from the corona radiata voxels, **a**, **a'** superimposed on their fitted model functions (gray lines). Note: *(a)* spectral resolution; *(b)* signal-to-noise ratio in these 0.75 cm^{3} voxels; and *(c)* the fidelity of the fitting procedure.

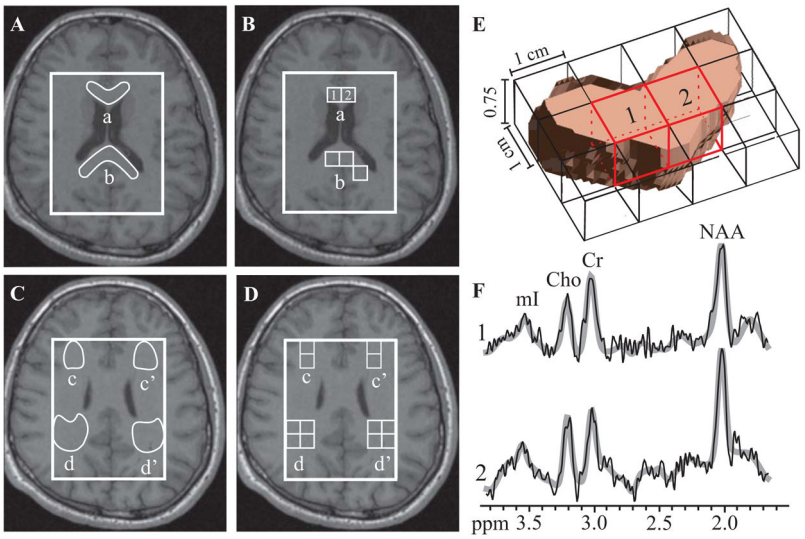

Fig. 2.

Left, top (**A**, **B**): Patient #9's axial T1-weighted MPRAGE overlaid with the manually outlined genu (**a**) and splenium (**b**) of the CC (**A**); and their corresponding partial volume-controlled voxels (**B**). Note almost complete absence of GM and CSF in these voxels, increasing the accuracy of the measurement. Left, bottom (**C**, **D**): Manually outlined bilateral frontal (**c**, **c'**) and occipital (**d**, **d'**) WM and their corresponding voxels. Right, top: (**E**) 3D rendering of the segmented genu within one, 0.75 cm-thick, ^{1}H MRSI slice, with voxels, indicated "1" and "2" on **B**. Note: these voxels comprise mostly genu tissue, due to the minimal tissue mask requirement and GM/CSF partial volume control. Right, bottom: (**F**) The spectra from the genu voxels in **E** with their fitted function (gray lines). Note that despite the proximity of frontal sinuses which can degrade spectral quality, there is only slight increase in linewidth compared to spectra distal to sources of magnetic susceptibility, *e.g.,* corona radiata (*cf.* Fig. 1). The increase does not affect the quantification or degrade the ability to resolve Cr from Cho at 3.0 and 3.2 ppm.

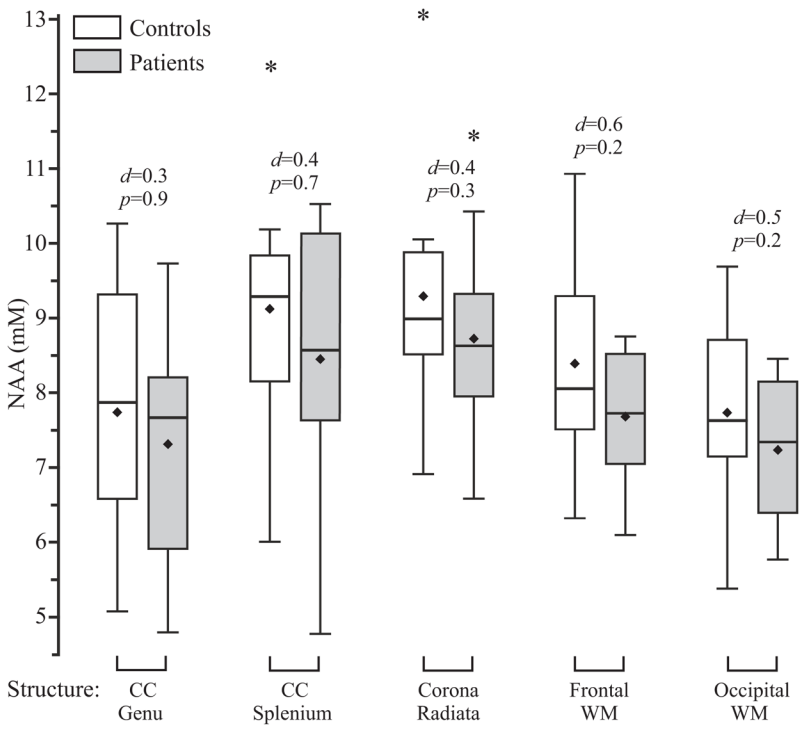

Fig. 3.

Box plots showing the 1st, 2nd (median), and 3rd quartiles (box), ±95% (whiskers), means (♦) and outliers (*) of the NAA absolute concentration distributions of the controls and patients with PCS mTBI for each WM ROI. Above each box plot pair are the *p* value from the analysis of covariance and the Cohen's *d* value as a measure of the effect size. Note that (*a*) despite lack of significant differences for any WM ROI, for each case the median (and mean) of the patients' NAA concentration is *lower* than the controls'; and (*b*) the Cohen's *d* values are all within a relatively narrow range, from 0.3 (genu) to 0.6 (frontal WM). Since the patients' average *global* WM NAA level was significantly lower than their controls (14), these distributions seem to imply the presence of diffuse injury across all WM ROIs which is, however, beneath the sensitivity threshold of the ^{1}H MRSI regional analysis.

Table 1.

Patient demographics, clinical data, symptoms and MRI findings, sorted by time from injury.

Patient	Age/ Sex	TBI Cause	GCS	LOC duration (minutes)	Days from mTBI	Symptoms[1]	T_1- and T_2-weighted imaging findings
1	40/M	Fall	15	3	3	V	None
2	41/M	Fall	15	<1	5	H, D, S	“
3	42/M	Fall	14	5	5	H, S, M	“
4	22/M	Assault	13	30	6	H	“
5	25/M	Assault	15	25	10	H	Right frontal convexity arachnoid cyst
6	32/M	Assault	15	2	17	H, D, S, M	None
7	23/M	Assault	15	30	18	H, D, M	“
8	18/M	Ped/Auto	15	15	19	H, D, M	“
9	51/M	MVA	14	30	19	H	Few punctate foci of abnormal T2 hyperintensities in frontal and parietal lobe subcortical WM with nonspecific etiology
10	37/M	Fall	15	2	20	H, D	None
11	51/F	Bike fall	14	30	20	H, D, S	Stable right cerebellopontine angle arachnoid cyst
12	28/F	Bike/Auto	15	20	29	H, D, S	None
13	32/F	Fall	15	1	43	D, M	“
14	44/F	Ped/Auto	15	<1	54	D, M	“
15	50/M	Fall	15	<1	55	H, D, S, M	“

GCS - Glasgow Coma Scale

LOC - loss of consciousness

[1] D - dizziness, H - headache, M – memory deficits, S - sleep disturbance, V - blurred vision.

Table 2.

Metabolic concentrations (average±standard deviation) in millimolar (mM) in each WM ROI within controls (C) and patients (P)

		Cohort	*Voxel number*	*Concentration (mM)*			
				NAA	**Cr**	**Cho**	**mI**
Corpus Callosum	Genu	C	3±1	7.7±1.6	5.2±2.1	1.5±0.5	5.2±1.0
		P	2±1	7.3±1.5	6.2±1.2	1.6±0.4	5.3±1.6
		p value		0.88	0.20	0.71	0.71
	Splenium	C	4±2	9.1±1.6	4.2±1.2	1.3±0.3	4.8±1.1
		P	4±2	8.4±1.7	4.4±0.7	1.3±0.2	5.0±1.0
		p value		0.73	0.75	0.96	0.37
Corona Radiata		C	6±3	9.3±1.5	6.5±1.3	1.9±0.4	5.6±1.2
		P	6±4	8.7±1.3	6.2±0.9	1.8±0.2	5.4±1.1
		p value		0.31[1]	0.40	0.30[1]	0.57
Frontal WM		C	2±1	8.4±1.5	5.9±1.5	1.8±0.3	5.6±1.2
		P	3±2	7.7±0.9	5.9±1.2	1.8±0.4	6.4±1.7
		p value		0.20	0.97	0.84	0.22[1]
Occipital WM		C	3±1	7.7±1.3	4.8±1.0	1.5±0.3	5.1±1.1
		P	5±2	7.2±0.9	4.9±0.9	1.6±0.3	5.5±0.8
		p value		0.20	0.96	0.55	0.39[1]

Shown for each ROI is the number of voxels (average±standard deviation) used for calculating the corresponding concentrations.

The *p* values are from the ANCOVA comparing patients to controls in terms of their metabolite concentrations in each ROI.

[1] *p* value was derived from an analysis based on ranks due to rejection of the assumption of normality.